scientific reports

OPEN Mixed convection flow of an electrically conducting viscoelastic fluid past a vertical nonlinearly stretching sheet

Ahmad Banji Jafar[1,2], Sharidan Shafie[2], Imran Ullah[3], Rabia Safdar[4], Wasim Jamshed[5✉], Amjad Ali Pasha[6], Mustafa Mutiur Rahman[7], Syed M. Hussain[8], Aysha Rehman[9], El Sayed M. Tag El Din[10] & Mohamed R. Eid[11,12]

The study of hydromagnetic mixed convection flow of viscoelastic fluid caused by a vertical stretched surface is presented in this paper. According to this theory, the stretching velocity varies as a power function of the displacement from the slot. The conservation of energy equation includes thermal radiation and viscous dissipation to support the mechanical operations of the heat transfer mechanism. Through the use of an adequate and sufficient similarity transformation for a nonlinearly stretching sheet, the boundary layer equations governing the flow issue are converted into a set of ordinary differential equations. The Keller box technique is then used to numerically solve the altered equations. To comprehend the physical circumstances of stretching sheets for variations of the governing parameters, numerical simulations are made. The influence and characteristic behaviours of physical parameters were portrayed graphically for the velocity field and temperature distributions. The research shows that the impact of the applied magnetic parameter is to improve the distribution of the viscoelastic fluid temperature and reduce the temperature gradient at the border. Temperature distribution and the associated thermal layer are shown to have improved because of radiative and viscous dissipation characteristics. Radiation causes additional heat to be produced in liquid, raising the fluid's temperature. It was also found that higher velocities are noticed in viscoelastic fluid as compared with Newtonian fluid (i.e., when K = 0).

A stretchable surface is an area that is supported at one end and moves in response to a tug at that end. Melted material is extracted from the slit and extended to the desired size while making sheets. As a result, the characteristics of a product made via industrial extrusion will rely on the speeds at which the sheet is stretched and cooled. However, many industrial processes, including the manufacturing of glass fibre and paper, metal spinning, strengthening of copper wires, and hot rolling, include the analysis of laminar flow across a stretched surface. There are several possible methods to define the velocity where the sheet is pulled from the emulsion slit, including linear, exponential, and nonlinear. In reality, many writers have looked at the flow of a linearly stretching sheet, for instance[1–8]. A nonlinear stretching sheet is used in several real-world scenarios. In light of this, it is frequently required to assume that the velocity of the sheet varies nonlinearly as a function of space from the slit.

[1]Department of Mathematics, Kebbi State University of Science and Technology, Aliero, P.M.B. 1144 Birnin Kebbi, Kebbi State, Nigeria. [2]Present address: Department Mathematical Sciences, Faculty Sciences, Universiti Teknologi Malaysia, Skudai, 81310 Johor Bahru, Johor, Malaysia. [3]College of Civil Engineering, National University of Sciences and Technology, Islamabad 44000, Pakistan. [4]Department of Mathematics, Lahore College for Women University, Lahore 54000, Pakistan. [5]Department of Mathematics, Capital University of Science and Technology (CUST), Islamabad 44000, Pakistan. [6]Aerospace Engineering Department, King Abdulaziz University, Jeddah 21589, Saudi Arabia. [7]Mechanical Engineering Program, Physical Science and Engineering Division, King Abdullah University of Science & Technology, Thuwal, ON 23955, Saudi Arabia. [8]Department of Mathematics, Faculty of Science, Islamic University of Madinah, Medina 42351, Saudi Arabia. [9]Department of Mathematics, University of Gujrat, Gujrat 50700, Pakistan. [10]Electrical Engineering, Faculty of Engineering and Technology, Future University in Egypt, New Cairo 11835, Egypt. [11]Department of Mathematics, Faculty of Science, New Valley University, Al-Kharga 72511, Al-Wadi Al-Gadid, Egypt. [12]Department of Mathematics, Faculty of Science, Northern Border University, Arar 1321, Saudi Arabia. ✉email: wasiktk@hotmail.com

1

We concentrate on nonlinear stretching sheets in this study. As a result, external flow control mechanisms, such as a magnetic field, are required to assure the correct feature. One field of research that combines the mechanics of fluids with some electromagnetic aspects to describe the transport phenomena in an electrically conducting fluid is magnetohydrodynamic (MHD) fluids, a branch of fluid mechanics that involves the analysis of electrically conducting fluids. The performance of fluid flow and heat transfer phenomena is influenced, controlled, and regulated by the existence of a magnetic field inside the fluid. It also has a substantial impact on solar physics, bioengineering, heat and mass transfer, metal, high thermal plasmas, MHD power generators, MHD reactors, thermal insulation, turbines, nuclear reactors coolant, and electronic packages, among other fields[9]. The variation of radiation and heat generation/absorption on MHD viscoelastic fluid flow via a stretched surface were examined by Datti et al.[10]. According to their findings, the existence of a magnetic field in the fluid causes a high rate of heat transmission, which improves heat transfer at the surface. Similar research is conducted by Abel et al.[11] on the magnetohydrodynamic flow of viscoelastic fluid caused by a stretched surface. They noticed that as the magnetic parameter improves, the speed of the flow field reduces. This is brought on by a drag force that seeks to impede fluid flow and lower its velocity, known as the Lorentz force. Sharada[12] examined the effect of a magnetic field on a steady flow of viscoelastic fluid. The author reveals that the Lorentz force gains more strength with the increased values of a magnetic parameter. Kumar and Sivaraj[13] also examined the magnetohydrodynamic natural convective flow of Walters' B viscoelastic fluid over a flat and vertical cone contained in a porous media.

In addition to exhibiting both viscosity and elasticity, one category of non-Newtonian fluids with dual effect features is viscoelastic fluid (i.e., heat transfer reduction and drag reduction properties)[14], which contributes to a wide range of applications in the polymer industry. Manufacture of paper, fibre glass, dyes, films, extraction processes, copper wire thinning and hardening, synthetic fibre and plastic film processing, drawing of plastic sheet, cooling of metallic chips, and food processing are all included in this[15]. In the process engineering of oil reservoirs, bio-engineering, the chemical industry, and nuclear technology, viscoelastic fluid is also crucial. Physically, the behaviour of viscoelasticity helps in depressing or enhancing the rate of the heat transfer process. However, it relies on the kinematic properties of the velocity field being studied as well as the heat exchange direction. Studying viscoelastic fluid and transport of heat adjacent to the continuous moving surface is an essential area of research as it helps in determining the desired and favourable output in most industrial and engineering processes. For this purpose, Abel[16] carried out heat transfer analysis in electrically conducting flow of viscoelastic fluid induced via non-isothermal linear stretching surface in the presence of heat generation and found that the temperature distribution within the boundary region reduces with an upsurge in viscoelasticity. The free conductive flow of Walters' B viscoelastic fluid via movable flat plates and vertical cones in the presence of varying electric conductivity was also examined by Sivaraj and Kumar[17]. Their research revealed that the magnetic field and varied electric conductivity had a substantial impact on the viscoelastic flow.

Furthermore, the numerical solution of a viscoelastic fluid passing a flat plate was achieved by Maryam et al.[18]. They used a second-order parallelized finite volume method and noticed that the drag coefficient at the boundary of viscoelastic fluids is lesser as compared to that of Newtonian fluids. Similarly, the impact of a magnetic field on two kinds of viscoelastic fluids produced by a stretched sheet was theoretically examined by Cortell[19]. According to his observations, the viscosity is greater in the second-grade fluid when compared to Walter's B liquid. Mustapha[20] examined the analytical solution of viscoelastic fluid generated by a nonlinearly stretching sheet by employing the method of homotopy analysis. The impact of viscous dissipation on the viscoelastic fluid flow caused by a vertical nonlinear stretching sheet was quantitatively examined by Jafar et al.[21] while Seth et al.[22] investigated the influence of velocity slip on the Dufour and Soret phenomena of MHD viscoelastic fluid created by a nonlinearly stretched surface. It was found that the viscoelasticity parameter reduces the fluid's temperature. Recently, Megahed et al.[23] examined the variations of viscous dissipation and variable fluid properties on the transport phenomenon of magnetohydrodynamic viscoelastic fluid. They discovered that as the viscosity and viscoelasticity parameters increase, the sheet velocity also increases. The influence of chemical reaction on Buongiorno's nanofluid model of viscoelastic fluid via a nonlinear stretched surface has been quantitatively examined by Nadeem et al.[24].

The thermophysical characteristics of fluid are subtly connected to the phenomena of heat transport systems. Indeed, the increasing demands to enhance heat dissipation, and cooling/heating processes as well as saving energy, time, and cost of production in the industrial system has been a challenge to many engineers and scientists. However, the analysis of boundary layer flow and heat transport, which happens when a heated surface moves continuously over a static fluid, has several technical uses in engineering and industrial production because it is crucial in determining the properties of the process's end product. This involves the process of extrusion of hot plastic and metals, continuous casting, hot rolling, and production of glass fiber and paper[25]. Convective heat transfer is usually the heat transfer process that exists in the presence of a fluid motion on a solid surface. Convective heat transfer is divided into two or three categories, which in turn aid the transfer of heat. The first category, which is usually called natural or free convection, arises due to the natural buoyancy forces (i.e. density gradient). The second category, which is usually called forced convection, arises due to the pressure differences and the last category occurs in a situation where the free convection is accompanied by the external force. In this case, mixed convection flow is the term for the type of heat transfer that results from the combined action of free and forced convection[26].

Much emphasis has been paid to the investigation of mixed convective flow along a rigid plate lately because it is essential for a variety of applications, including the electronic cooling devices by fans, the cooling of nuclear reactors during an unexpected failure, the placement of heating systems in minimal-velocity environments, solar cells, and others. When the flow is horizontal, the buoyancy force is disregarded in the analysis of flow across hot surfaces. However, the buoyant force has a substantial impact on the flow field for vertical or inclined surfaces. To achieve this, Lloyd and Sparrow[27] used the local similarity technique to solve the convective heat transfer flow caused by a vertical plate, showing that the numerical simulations included both forced and mixed convection.

Figure 1. Schematic figure of a stretching sheet in viscoelastic fluid.

Prasad et al.[28] probed the impact of varying fluid characteristics on the mixed convection heat transport via a nonlinearly stretching sheet. Soret and Dufour effects on the convective flow of viscoelastic fluid over a stretched sheet encased in a porous medium were also studied by Jena et al.[29]. Furthermore, Hayat et al.[30] also examined a viscoelastic Walters-B nanofluid mixed convection flow via a nonlinear vertical stretched surface with varying thickness.

The emission of energy in the form of electromagnetic waves is referred to as radiation. Through this method, energy can be conveyed as heat, energy, or light. Numerous fluid parameters are altered when such emission results from fluid flow[24]. The thermal radiation effect is important for adjusting a system's temperature, modifying the pace of heat transport, and managing the thermal boundary layer. To explore the influence of thermal radiation on the natural convective flow Powell-Eyring nanofluid via a cylinder, Kumaran et al.[31] conducted an investigation. They observed that a reduction in heat transfer processes results from an increase in the radiation parameter. Many studies, like Raja et al.[7], Datti et al.[11], and Ahmad et al.[15], have considered the impact of radiant heat on boundary layer flow induced by a nonlinearly stretching sheet because of its significance in controlling and maintaining the system's temperature.

One must also consider the viscous dissipation effect in addition to the impacts of magnetic and thermal radiation on the flow field. The energy created by the work done as a result of frictional heating between fluid layers is known as viscous dissipation. By acting as an energy source, the heat energy generated modifies temperature distributions, which in turn affects fluid temperature and heat transfer rates. Greater gravitational fields, massive planets, denser space gases, and geological phenomena all result in viscous dissipation[32]. Several authors have considered viscous heating effects on boundary layer flows, such as Hsiao[33], Reddy et al.[34], Yaseen et al.[35], and Jhahan et al.[36].

The primary objective of the current study is to find a numerical solution for the flow of a viscoelastic fluid through a mixed convection boundary layer as a consequence of the cumulative impact of a uniform magnetic field, viscous dissipation, and thermal radiation via a vertical sheet that is not linearly stretching. By employing an unconditionally stable Keller box strategy[37] to analyse a group of linked nonlinear ordinary differential equations, the non-similar solutions of the modified equations are achieved numerically. This method has been widely used by many researchers like Kumaran et al.[38] and Hayath et al.[39] in dealing with parabolic differential equations. For more details see[40,41].

Governing equations.   We take into account a viscoelastic fluid flowing in mixed convective two-dimensional magnetohydrodynamic flow across a stretched sheet, as seen in Fig. 1. The extrusion slit, where the sheet is drawn, serves as the system's point of origin. The x-axis is drawn along the continuously extending surface and faces forward. The sheet is parallel to the y-axis. The sheet is subjected to a perpendicular $B(x)$ magnetic field. The sheet velocity, $U_w(x) = ax^n$ is assumed to vary as a nonlinear function of the distance from the slit, where $a > 0$ is the stretching rate and n is a nonlinear stretching parameter. The temperature of the fluid, $T_w(x) = T_\infty + T_0 x^{2n-1}$ is also considered as a nonlinear function of the distance from the slit, where T_0 is a positive constant and T_∞ is the ambient temperature of the fluid. Thus, using the conventional boundary layer approximation, the viscoelastic fluid equations governing the momentum and energy equations may be expressed as follows[11,21].

$$\frac{\partial u}{\partial x} + \frac{\partial v}{\partial y} = 0, \tag{1}$$

$$u\frac{\partial u}{\partial x}+v\frac{\partial u}{\partial y} = v\frac{\partial^2 u}{\partial y^2}-\frac{k_0}{\rho}\left(u\frac{\partial^3 u}{\partial x\partial y^2} + \frac{\partial u}{\partial x}\frac{\partial^2 u}{\partial y^2} - \frac{\partial u}{\partial y}\frac{\partial^2 u}{\partial x\partial y} + v\frac{\partial^3 u}{\partial y^3}\right)-\frac{\sigma}{\rho}B^2(x)u+g\beta(T - T_\infty), \qquad (2)$$

$$\rho c_p\left(u\frac{\partial T}{\partial x} + v\frac{\partial T}{\partial y}\right) = k\frac{\partial^2 T}{\partial y^2} - \frac{\partial q_r}{\partial y} + \mu\left(\frac{\partial u}{\partial y}\right)^2 + \sigma B^2(x)u^2, \qquad (3)$$

where u and v are the fluid flow's velocity components along x and y directions, μ, v, k_o, ρ, σ, g, β, ρc_p, q_r and k are respectively, the viscosity, kinematic viscosity, material constant, fluid density, electrical conductivity, gravitational acceleration, thermal expansion coefficient, heat capacitance, radiative heat flux, and thermal conductivity of the fluid. The boundary conditions for the governing Eqs. (1)–(3) take the form

$$\left.\begin{array}{l} u = U_w(x) = ax^n, v = 0, T(x) = T_w(x) = T_\infty + T_0 x^{2n-1} \ a \ ty = 0, \\ u \to 0, \frac{\partial u}{\partial y} \to 0, T \to T_\infty \ as \ y \to \infty, \end{array}\right\} \qquad (4)$$

where the subscripts w and ∞ refer to stretching at the wall and free stream, respectively. The magnetic field $B(x)$ is considered to have the form in order to simplify the similarity solution.

$$B(x) = B_0 x^{2n-1}, \qquad (5)$$

where B_0 is a constant. In order to ensure that the generated magnetic field is minimal, it is also expected that the liquid has weak electrical conductivity. The Rosseland approximation is used to simulate the flow of thermal radiation[11,31]. The heat flux is assumed to be proportionate to the temperature difference in this approximation, and heat moves from the hard surface to the liquid. In light of this, the radiative heat flux q_r is written in the following form

$$q_r = -\frac{4\sigma^*}{3k^*}\frac{\partial T^4}{\partial y}, \qquad (6)$$

where σ^* signifies Stefan-Boltzmann constant and k^* symbolizes the rate. Assuming that T^4 can be represented as a linear function of temperature $T^4 \equiv 4T_\infty^3 T - 3T_\infty^4$ and that the temperature variations within the fluid flow are suitably low. With this, Eq. (6) can be written as

$$\frac{\partial q_r}{\partial y} = -\frac{16\sigma^* T_\infty^3}{3k^*}\frac{\partial^2 T}{\partial y^2}. \qquad (7)$$

Substituting Eq. (7) into Eq. (3) gives

$$\rho c_p\left(u\frac{\partial T}{\partial x} + v\frac{\partial T}{\partial y}\right) = k\frac{\partial^2 T}{\partial y^2} + \frac{16\sigma^* T_\infty^3}{3k^*}\frac{\partial^2 T}{\partial y^2} + \mu\left(\frac{\partial u}{\partial y}\right)^2 + \sigma B^2(x)u^2. \qquad (8)$$

In order to simplify the governing equations of the present problem, the following specified similar quantities are introduced.

$$\eta = y\sqrt{\frac{(n + 1)U_w}{2av}}, \quad \psi(x,y) = \sqrt{\frac{2avU_w}{(n + 1)}}f(\eta), \quad \theta(\eta) = \frac{T - T_\infty}{T_w - T_\infty}. \qquad (9)$$

where η represents the similarity variable, $f(\eta)$ is the dimensionless stream function, $\theta(\eta)$ corresponds to the non-dimensional temperature and the stream function $\psi(x,y)$ satisfies the continuity Eq. (1) such that the components of the velocity u and v are defined as

$$u = \frac{\partial\psi}{\partial y} \ \text{and} \ v = -\frac{\partial\psi}{\partial x}. \qquad (10)$$

By using Eqs. (5) and (9), Eqs. (2), (4), and (8) can be transformed into the system of ordinary differential equations

$$f'''+ff'' -\left(\frac{2n}{n + 1}\right)f'^2 -K\left\{(3n - 1)f'f''' - \left(\frac{3n - 1}{2}\right)f''^2 - \left(\frac{n + 1}{2}\right)ff^{iv}\right\}-\left(\frac{2}{n + 1}\right)\left(Mf' - \lambda\theta\right) = 0, \qquad (11)$$

$$\frac{1}{Pr}\left(1 + \frac{4}{3}R\right)\theta'' + f\theta' - \left(\frac{2(2n - 1)}{n + 1}\right)f'\theta + M(f')^2 + Ec(f'')^2 = 0, \qquad (12)$$

$$\left.\begin{array}{l} f(0) = 0, f'(0) = 1, \theta(0) = 1, \\ f'(\infty) \to 0, f''(\infty) \to 0, \theta(\infty) \to 0. \end{array}\right\} \qquad (13)$$

The non-dimensional parameters that appeared in Eqs. (11)–(13) are the viscoelastic parameter K, magnetic parameter M, mixed convection parameter λ, Prandtl number Pr, radiation parameter R, and Eckert number Ec. These parameters are respectively defined as

$$K = \frac{k_0 a^{1/n} U_w^{(n-1)/n}}{\rho \nu}, \ M = \frac{\sigma B_0^2}{\rho a}, \ \lambda = \frac{g\beta(T_w - T_\infty)}{a^{2/n}\nu U_w^{(n-2)/n}}, \ Pr = \frac{\rho \nu C_p}{k}, \ R = \frac{4\sigma^* T_\infty^3 T}{kk^*} \text{ and } Ec = \frac{U_w^2}{C_p(T_w - T_\infty)}.$$

(14)

Upon formulation of the governing equations for mixed convective viscoelastic flow due to a nonlinearly stretching sheet with the aforementioned assumptions. Then, we develop the expressions for important physical parameters, which are of engineering interest. These parameters are the skin friction coefficient C_f and the local Nusselt number Nu_x. They provide examples of the stretched surface drag and rate of wall heat transfer. Then, the wall shear stress τ_w is determined by

$$\tau_w = \left[\mu \frac{\partial u}{\partial y} + k_0 \left(u\frac{\partial^2 u}{\partial x \partial y} + \nu \frac{\partial^2 u}{\partial y^2} - 2\frac{\partial u}{\partial y}\frac{\partial \nu}{\partial y} \right) \right]_{y=0}.$$

(15)

The non-dimensional skin friction coefficient is defined by

$$C_f = \frac{\tau_w}{\rho U_w^2}.$$

(16)

The skin friction coefficient in terms of transformation variables (9) and (10) can be obtained as

$$Re^{\frac{1}{2}} C_f = \left(\frac{n+1}{2}\right)^{\frac{1}{2}} \left[1 + K\left(\frac{7n-1}{2}\right)\right] f''(0).$$

(17)

The heat flux at the stretched surface may be calculated using

$$q_w = \left[-\left(k + \frac{16\sigma^* T_\infty^3}{3k^*} \right) \frac{\partial T}{\partial y} \right]_{y=0},$$

(18)

and the heat transfer coefficient is defined as

$$Re^{-\frac{1}{2}} Nu = -\frac{1}{k}\left(\frac{n+1}{2}\right)^{\frac{1}{2}} \left(1 + \frac{4}{3}R\right)\theta'(0),$$

(19)

where $Re = \frac{U_w x}{\nu}$ is the local Reynolds number.

Numerical explanation procedure. In the current study, we reduced the dimensional governing equations into a non-dimensional form using similarity variables. The set of transformed differential Eqs. (11), (12) and corresponding boundary conditions (13) were numerically solved using Cebeci and Bradshaw's Keller box method[37], an implicit finite difference technique. Selecting acceptable finite values of $\eta \to \infty$ is the method's crucial stage. Nevertheless, we begin with starting values for pertinent parameters in order to establish $f''(0)$ and $\theta'(0)$ for the boundary value problem represented by Eqs. (10), (11) before attempting to determine $\eta \to \infty$. Until the findings are rectified to the necessary precision of 10^{-5} level, the procedure is repeated. The drag force $f''(0)$ and Nusselt number $\theta'(0)$ were quantified numerically for each pair of sequential values. For a different set of physical factors, the values of η may vary.

The related boundary value problem presented by Eqs. (10), (11) is then numerically addressed using the Keller box approach once the proper value of η has been established. This method was designed specifically for the parabolic type of differential equations. In this method, the numerical solution is obtained by considering the step size of 0.02 with a five-decimal places criterion of convergence for accuracy. In fact, one needs to consider the following four basic procedures in using the method:

1. Re-written the transformed Eqs. (10), (11) with their corresponding boundary conditions (12) into a first-order system of equations.
2. Using the central difference method to convert the obtained first order equations into set finite difference equations.
3. Newton quasi-linearization method is then employed in solving the system of non-linear equations.
4. Block-matrix algorithm is finally used to solve the differential equations.

Results and discussion

To better comprehend the flow pattern, numerical figures for the temperature and velocity are generated for variations of non-dimensional factors, such as the nonlinear stretching parameter (n), viscoelastic parameter (K), magnetic field parameter (M), mixed convection parameter (λ), radiation parameter (R), viscous dissipation parameter (Ec) and Prandtl number (Pr). Additionally, the impact of these factors on non-dimensional Nusselt number and skin friction is explored. An investigation of the mixed convection flow of a viscoelastic fluid with combined effects of viscous dissipation and radiation across a nonlinearly extending sheet has been done in this paper. The whole flow fields are studied using the boundary layer idea in order to provide a set of linked

n	Pr	Hsiao[33]	Present results
1.5	1	0.8240	0.82411
3.0	1	0.9142	0.91430
10	1	1.0018	1.00000
1.5	2	1.2807	1.28079
1.5	5	2.1788	2.17897

Table 1. Comparative analysis of $-\theta'(0)$ obtained by the numerical technique with that of Hsiao[33] for numerous values of n and Pr. Fixing $K = M = \lambda = 0$ and $R = 0.2$, $Ec = 0.1$.
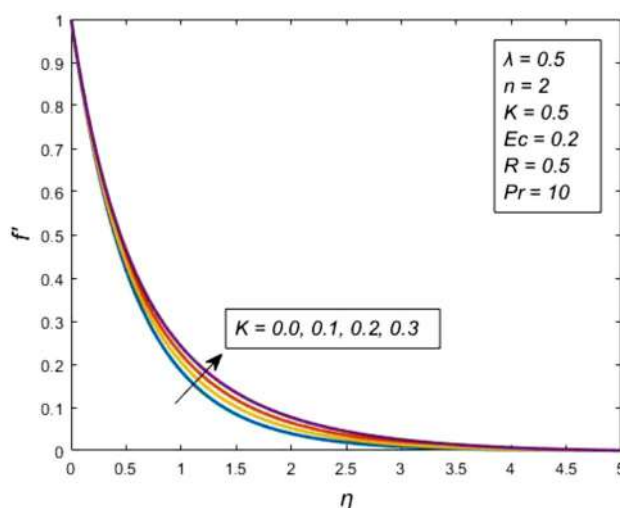
Figure 2. Impact of viscoelastic parameter K on the velocity profile.

momentum and energy equations that may be used to solve the problem. The appropriate similarity variables have been provided, which converts the momentum and energy equations into a couple of nonlinear ordinary differential equations, hence simplifying the governing partial differential equations into ordinary differential equations. The Keller box approach was then used to achieve the numerical results. The analysis of the parameters n, K, M, λ, R, Ec, and Pr effects on the velocity and temperature distributions were inferred from the data. The impact of these factors on non-dimensional heat transfer coefficient and skin friction is also examined in tabular form. Comparing the numerical solutions of heat transfer rate $(-\theta'(0))$ for various values of n and Pr by fixing $K = M = \lambda = 0$ and $R = Ec = 0.1$ with Hsiao[33] allowed for the determination of the numerical method's validity, as shown in Table 1. The comparison reveals good agreement, which supports the adoption of the Keller box approach.

Cooling is related to the heat transfer rate from the hot surface during numerous industrial manufacturing processes such as glass blowing, metal extrusion, glass fibre manufacture, and polymer extrusion. The primary goal in these types of issues is to limit the rate of heat transmission, which depends on the production method and the physical makeup of the issue at hand. Given this, Figs. 2, 3, 4, 5, 6, 7, 8 and 9, which illustrate the impacts of a viscoelastic, nonlinear stretching sheet, mixed convection, radiation parameter, Eckert and Prandtl numbers on the velocity $f'(\eta)$ and temperature $\theta'(\eta)$ profiles are shown after the tables and their comments.

Figures 2 and 3 are displayed to see the influence of viscoelastic parameter K on the velocity and temperature profiles. From this plot, it is evident that rising viscoelastic parameter K values cause the velocity across the boundary layer to rise. This implies that the fluid flow velocity increases as the viscoelastic parameter increases. This practically indicates that the characteristics of fluid flow in viscoelastic fluids may be influenced by modifying the change in the K. It is also obvious from Fig. 3 that to increase the magnitude of K is to decrease the temperature profile. When the dimensionless temperature profile is lower, K value is higher.

As a result, the fluid's heat may be readily removed from it by the viscoelasticity force, which has positive effects for more viscoelasticity. The reason for this is that while the thermal boundary layers are reduced as the viscoelastic effects become more pronounced, which results in a higher rate of heat transfer among the viscoelastic fluid and sheet surface, the material variables, which have an inverse relation with the fluid viscosity, are what causes the increase in a momentum boundary layer.

The behaviour of nonlinear stretching parameter n on velocity profile is seen in Fig. 4. It demonstrates this since an increase in n causes the stretching sheet to increase. In actuality, stretching velocity rises because n is increased, which causes the viscoelastic fluid to deform more. As n increases, the boundary layer thickness eventually thickens. Where $n = 1$ results correspond to linear stretching sheet and for $n > 1$ results correspond
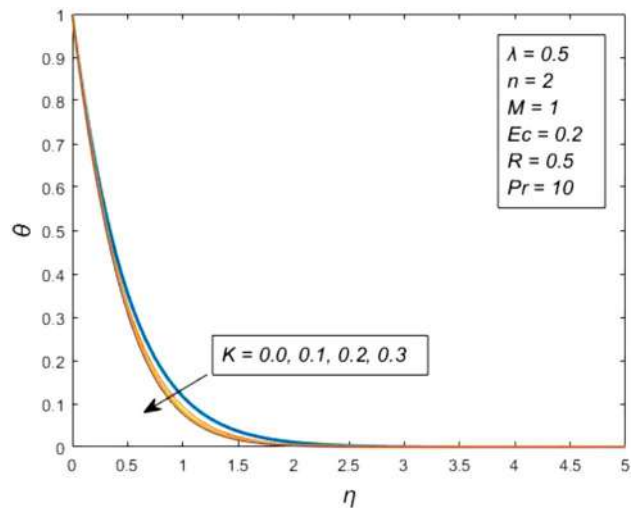
Figure 3. Impact of viscoelastic parameter *K* on the temperature profile.
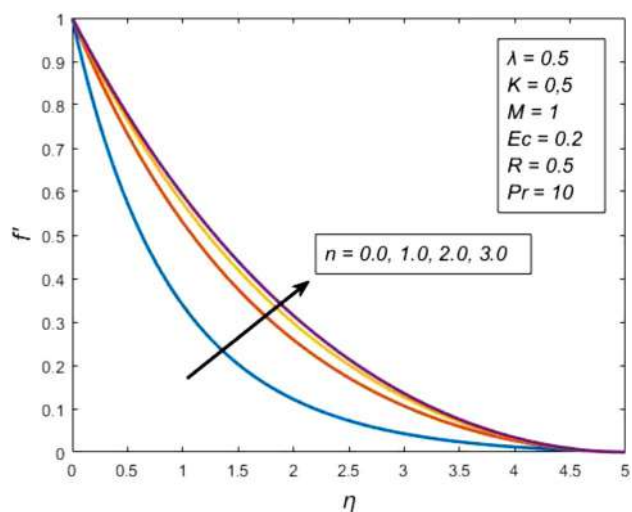
Figure 4. Impact of nonlinear stretching sheet parameter *n* on the velocity profile.
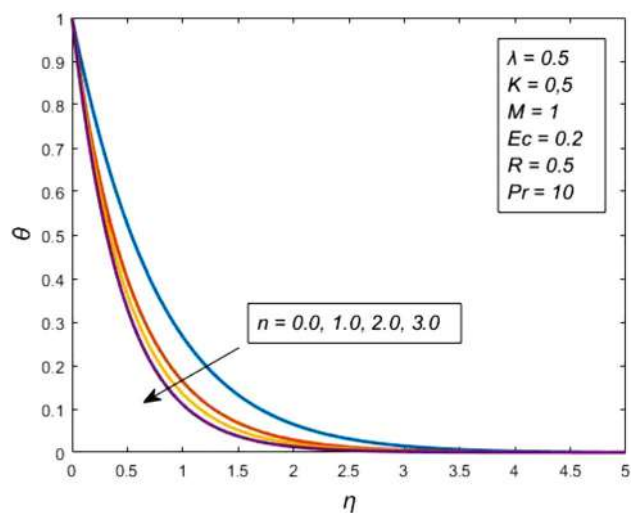
Figure 5. Impact of nonlinear stretching sheet parameter *n* on the temperature profile.
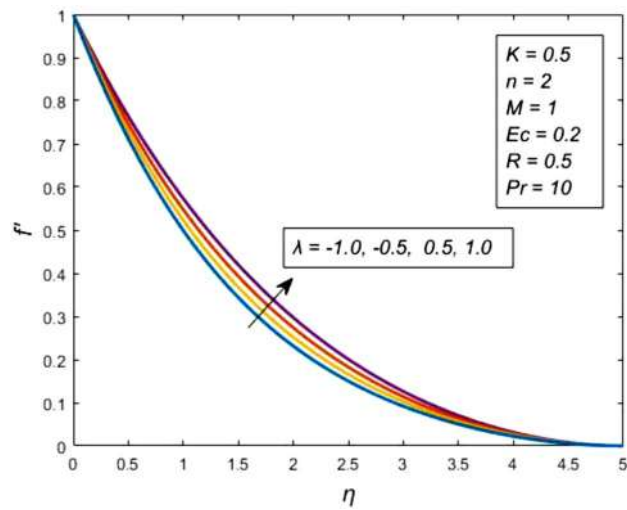
Figure 6. Impact of mixed convection parameter λ on the velocity profile.
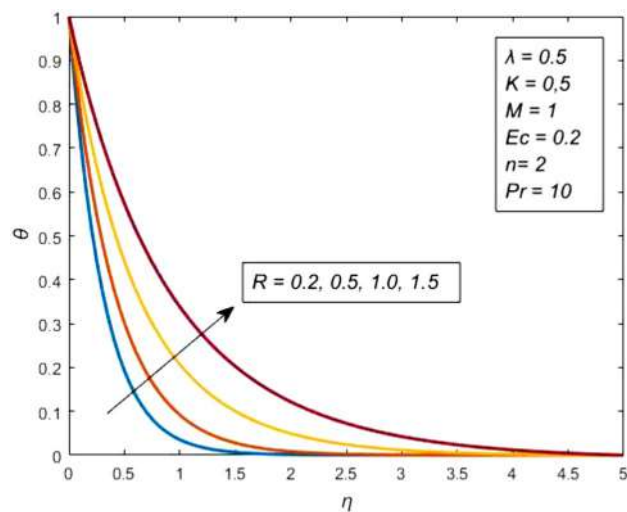
Figure 7. Impact of radiation parameter R on the temperature profile.
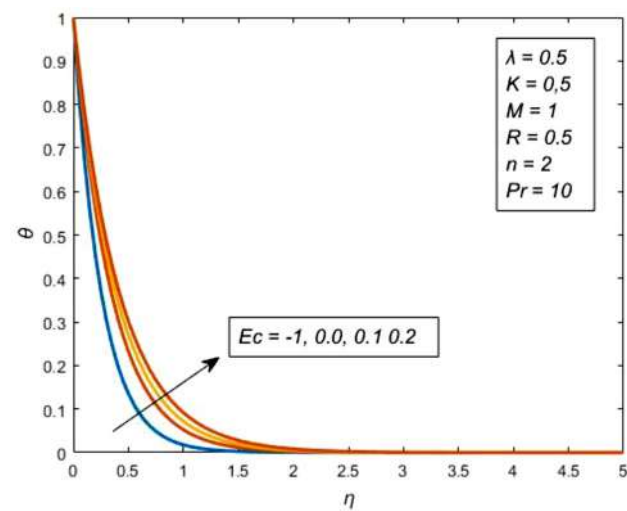
Figure 8. Impact of Eckert number Ec on the temperature profile.

 8
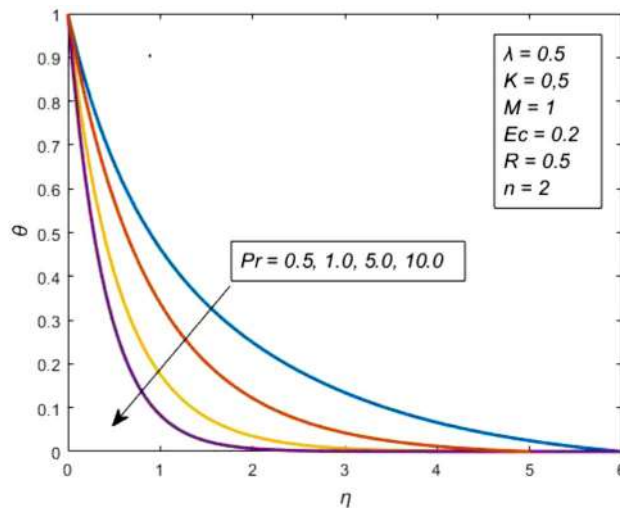
Figure 9. Temperature profile for various values of Prandtl number *Pr*.

to nonlinearly stretching surface. Studies comparing $n = 1$ and $n > 1$ show that when $n > 1$ (i.e., a nonlinearly stretching sheet) is present within the stretching boundary layer as opposed to the linear stretching sheet situation, velocity magnitude considerably rises. The behaviour of nonlinear stretching parameter *n* on temperature profile is depicted in Fig. 5. Practically, it is known that the heat transfer from a thinner region will be greater than that of a thicker region. The stretching rate of the surface rises as *n* grows because more energetic particles are delivered to the flow; as a response, the thickness of the sheet decreases, which improves the rate of heat transmission. Significantly, the thermal boundary layer gets thinner for larger values of *n*.

Figure 6 illustrates the effects of mixed convection parameters on the velocity profile. It is revealed that strengthening the value of λ enhances the buoyancy effect in the flow regime and hence, the velocity profile grows. The buoyancy-assist flow $(\lambda > 0)$ has a higher velocity profile than the buoyancy-resisting flow $(\lambda < 0)$, and vice versa. This effect is caused physically by buoyancy force, which behaves as a pressure gradient and propels or depreciates the fluid in the boundary layer, in turn raising the velocity profile. The effects λ on the temperature profile show that it has a minimal impact on the temperature profile, hence no graph is presented.

Figure 7 shows the characteristics of radiation parameter *R* with the temperature profile. It is observed from this graph that the thermal field increased with the increase in *R*. More heat is transferred to the working liquid via the radiation phenomena because the radiation parameter is inversely related to the mean absorption coefficient. A higher radiation parameter value causes k^* to decline, which raises the temperature. As a result, the rate of thermal convection into the fluid increases, as does the deviation of radiative heat flow. The increased thermal heat transfer is advantageous for the development of thermal boundary layers. As a result, the thermal layer thickens.

Whether the sheet is being heated or cold affects how important viscous dissipation is. Due to the viscoelastic nature of the fluid, we used for the analysis, frictional heating caused by viscous dissipation will be used to store the energy in the fluid. Figure 8 displays the variation of viscous dissipation which is represented in terms of Eckert number *Ec* on the temperature profile. When a fluid is heated, viscous dissipation $(Ec > 0)$ causes the temperature to rise, however when a fluid is cooled, we see the opposite behaviour regarding the temperature profile when $(Ec < 0)$. On the other hand, due to the effect of viscous dissipation, the existence of viscous dissipation in the energy equation works as an internal heat source, causing the dimensionless temperature to increase at $Ec > 0$ in comparison to $Ec < 0$. Due to frictional heating, *Ec* produces more heat in the liquid when it is physically bigger. Consequently, a hike in temperature is seen.

The trend of the Prandtl number *Pr* on the temperature profile is seen in Fig. 9. Fluids experience both conduction and convection. They can be viewed as competing with one another in terms of transmitting heat because the temperature differential is decreased by both processes, which transfer heat. Fluids come in a variety of forms, including mercury, oil, water, air, and many others. Various fluids exhibit different rates of conduction and convection. Conduction can sometimes take control. Convection occasionally takes control. One metric that can help indicate which process will prevail is the Prandtl number. If a fluid is more viscous, the Prandtl number is higher and the heat transfer will be less convective since *Pr* is the ratio of momentum to thermal thermal diffusivity. The thermal boundary layer thickness and temperature distribution are reduced as a result of poorer thermal diffusivity, which is associated with larger values of *Pr*.

For various values of the magnetic parameter M and viscoelastic parameter *K*, the values of the skin friction coefficient are shown in Table 2. The numbers in the table show that increasing the values of the skin friction coefficient is a result of strengthening the values of *M*. This implies that when the magnetic field's strength increases, the fluid flow will face significant resistance or drag. This happens because a higher magnetic field causes a Lorenz drag, which raises the value of the drag force. In practice, this means that raising the intensity of the magnetic field might be used to limit the fluid flow rate, which could be a beneficial method for managing the final qualities of the extrusion properties. Similar to this, it is observed that when the values of the viscoelastic parameters *K* grow,

M	K	$f''(0)$
0	0.2	1.39209
1	0.2	1.63028
2	0.2	1.92373
3	0.2	2.26984
4	0.2	2.69223
1	0.0	0.99381
1	0.1	0.78283
1	0.3	0.45123
1	0.5	0.41428
1	0.7	0.20281

Table 2. Numerical computation for drag force $-f''(0)$ with various values of M and K with $n = 2$, $\lambda = 0.5$, $R = 0.2$, $Ec = 0.1$, and $Pr = 10$.

M	R	Ec	$-\theta'(0)$
0	0.2	0.1	3.81352
1	0.2	0.1	3.47201
2	0.2	0.1	3.09209
3	0.2	0.1	2.81003
1	0	0.1	4.66732
1	0.5	0.1	3.59426
1	1.0	0.1	3.01694
1	1.5	0.1	2.37161
1	2.0	0.1	1.99023
1	0.2	0	3.85772
1	0.2	0.1	3.62598
1	0.2	0.2	3.59426
1	0.2	0.3	2.89809
1	0.2	0.4	1.73047

Table 3. Numerical values of Nusselt number $\theta'(0)$ for numerous values M, R, and Ec with $n = 2$, $K = 0.2$, $\lambda = 0.5$ and $Pr = 10$.

the magnitude values of $-f''(0)$ decrease. Since the power required to stretch a sheet is reduced by strengthening the value K, this result is significant in many industrial applications.

Table 3 displays how the non-dimensional heat transfer coefficient $-\theta(0)$ is affected by magnetic parameter M, radiation parameter R, and viscous dissipation parameter Ec. From the data in the table, it is clear that decreasing the value of any one of the three factors would decrease the value of the heat transfer coefficient. As a result, the heat transfer coefficient will decrease as the magnetic field's intensity increases, the fluid flow regime is exposed to radiative heat flux, and thermal energy from frictional heating caused by fluid movement is taken into account. This happens as a result of a sluggish heat transfer from the wall to the fluid caused by the magnetic field's reduction in fluid flow rate. The temperature of the fluid rises as a result of increased thermal radiation and viscous dissipation, which also slows heat transmission from the wall to the fluid. By strengthening the magnetic field and raising the fluid's temperature, it is possible to practically regulate the heat transfer across the stretched sheet's fluid interface. To help create a better cooling environment, radiation should be reduced to a minimum.

Conclusion

In the presence of an applied magnetic field, thermal radiation, and viscous dissipation, the mathematical model including mixed convection boundary layer flow of viscoelastic fluid and heat transfer phenomena across a nonlinearly stretching sheet has been investigated. When building heat transfer systems for diverse industrial applications, the rate of heat transmission is a key consideration. Depending on the applications, it may occasionally be necessary to raise or decrease the heat transfer rate to achieve better outcomes in the heating or cooling operations. Additionally, the findings are important since the material qualities of the wall rely on the pace of cooling or heating during the production of metal or polymer sheets. Therefore, an increase in temperature distribution and the associated thermal layer is caused by radiative and viscous dissipation. In reality, radiation causes more heat to be produced in liquids, raising their temperature. Radiation has an impact on heat transport and temperature distribution at high temperatures. Within the nonlinearly expanding boundary layer, opposing

transport phenomena are where the magnetic field dominates. The study also shows that the applied magnetic field parameter increases the temperature profile while decreasing the rate of heat transfer through the walls. The results also showed that the increment of the nonlinear stretching sheet parameter *n* increases the drag coefficient due to an improvement in momentum diffusivity, which is the cause of the low rate of heat transfer because the rate of heat transfer decreases with increasing boundary layer thickness.

The Keller-box method could be applied to a variety of physical and technical challenges in the future[42–52]. Some recent developments exploring the significance of the considered research domain are reported by[53–65].

Data availability

All data generated or analyzed during this study are included in this published article.

References

1. Crane, L. J. Flow past a stretching plate. *Zeitschr. Angew. Math. Phys. ZAMP.* **21**(4), 645–647 (1970).
2. Gupta, A. & Gupta, P. Heat and mass transfer on a stretching sheet with suction or blowing. *Can. J. Chem. Eng.* **55**(6), 774–746 (1977).
3. Andersson, H. I., Bech, K. H. & Dandapat, B. S. Magnetohydrodynamic flow of a power-law fluid over a stretching sheet. *Int. J. Nonlinear Mech.* **27**, 929–936 (1992).
4. Nayak, M. K., Akbar, N. S., Pandey, V. S., Khan, Z. H. & Tripathi, D. 3D free convective MHD flow of nanofluid over permeable linear stretching sheet with thermal radiation. *Powd. Technol.* **315**, 205–215 (2017).
5. Mahabaleshwar, U. S., Anusha, T. & Hatami, M. The MHD Newtonian hybrid nanofluid flow and mass transfer analysis due to super-linear stretching sheet embedded in porous medium. *Sci. Rep.* **11**(1), 1–17 (2021).
6. Uddin, Z., Vishwak, K. S. & Harmand, S. Numerical duality of MHD stagnation point flow and heat transfer of nanofluid past a shrinking/stretching sheet: Metaheuristic approach. *Chin. J. Phys.* **73**, 442–461 (2021).
7. Raja, M. A. Z., Shoaib, M., Hussain, S., Nisar, K. S. & Islam, S. Computational intelligence of Levenberg-Marquardt backpropagation neural networks to study thermal radiation and Hall effects on boundary layer flow past a stretching sheet. *Int. Commun. Heat Mass Transfer* **130**, 105799 (2022).
8. Nandi, S., Kumbhakar, B. & Sarkar, S. MHD stagnation point flow of Fe_3O_4/Cu/Ag-CH_3OH nanofluid along a convectively heated stretching sheet with partial slip and activation energy: Numerical and statistical approach. *Int. Commun. Heat Mass Transfer* **130**, 105791 (2022).
9. Pal, D., Mandal, G. & Vajravelu, K. MHD convection–dissipation heat transfer over a non-linear stretching and shrinking sheets in nanofluids with thermal radiation. *Int. J. Heat Mass Transf.* **65**, 481–490 (2013).
10. Datti, P. S., Prasad, K. V., Abel, M. S. & Joshi, A. MHD viscoelastic fluid flow over a non-i sothermal stretching sheet. *Int. J. Eng. Sci.* **42**, 935–946 (2004).
11. Abel, S., Joshi, M. & Sonth, R. M. Heat transfer in MHD viscoelastic fluid over a stretching surface. *Z. Angew. J. Math. Mech.* **81**, 691–698 (2001).
12. Sharada, K. Heat and mass transfer effects on MHD mixed convection flow of viscoelastic fluid with constant viscosity and thermal conductivity. *Heat Transfer* **51**(1), 1213–1236 (2022).
13. Kumar, B. R. & Sivaraj, R. MHD viscoelastic fluid non-Darcy flow over a vertical cone and a flat plate. *Int. Commun. Heat Mass Transfer* **40**, 1–6 (2013).
14. Yang, J., Li, F., Zhou, W., He, Y. & Jiang, B. Experimental investigation on the thermal conductivity and shear viscosity of viscoelastic-fluid-based nanofluids. *Int. J. Heat Mass Transf.* **55**(11–12), 3160–3166 (2012).
15. Ahmad, H., Javed, T. & Ghaffari, A. Radiation effect on mixed convection boundary layer flow of a viscoelastic fluid over a horizontal circular cylinder with constant heat flux. *J. Appl. Fluid Mech.* **9**(3), 1167–1174 (2016).
16. Abel, S. Heat transfer in MHD visco-elastic fluid flow over a stretching surface. *ZAMM J. Appl. Math. Mech.* **81**(10), 691–698 (2001).
17. Sivaraj, R. & Kumar, B. R. Viscoelastic fluid flow over a moving vertical cone and flat plate with variable electric conductivity. *Int. J. Heat Mass Transf.* **61**, 119–128 (2013).
18. Maryam, A. N., Ali, B., Moghadam, J. & Norouzi, M. A numerical study on viscoelastic boundary layer on flat plate. *J. Braz. Soc. Mech. Sci. Eng.* **42**(1), 11 (2020).
19. Cortell, R. A novel analytic solution of MHD flow for two classes of visco-elastic fluid over a sheet stretched with non-linearly (quadratic) velocity. *Meccanica* **48**(9), 2299–2310 (2013).
20. Mustafa, M. Viscoelastic flow and heat transfer over a non-linearly stretching sheet: OHAM solution. *J. Appl. Fluid Mech.* **9**, 1321–1328 (2016).
21. Jafar, A. B., Shafie, S. & Ullah, I. Magnetohydrodynamic boundary layer flow of a viscoelastic fluid past a nonlinear stretching sheet in the presence of viscous dissipation effect. *Coatings* **9**, 490 (2019).
22. Seth, G. S., Bhattacharyya, A. & Mishra, M. K. Study of partial slip mechanism on free convection flow of viscoelastic fluid past a nonlinear stretching surface. *Comput. Therm. Sci. Int. J.* **11**, 105–117 (2019).
23. Megahed, A. M. & Reddy, M. G. Numerical treatment for MHD viscoelastic fluid flow with variable fluid properties and viscous dissipation. *Indian J. Phys.* **95**(4), 673–679 (2021).
24. Nadeem, S. *et al.* Numerical computations for Buongiorno nano fluid model on the boundary layer flow of viscoelastic fluid towards a nonlinear stretching sheet. *Alex. Eng. J.* **61**(2), 1769–1778 (2022).
25. Al-Sanea, S. A. Convection regimes and heat transfer characteristics along a continuously moving heated vertical plate. *Int. J. Heat Fluid Flow* **24**(6), 888–901 (2003).
26. Aydin, O. & Kaya, A. MHD mixed convection of a viscous dissipating fluid about a vertical slender cylinder. *Desalin. Water Treat.* **51**(16–18), 3576–3583 (2013).
27. Lloyd, J. R. & Sparrow, E. M. Combined free and forced convective flow on vertical surfaces. *Int. J. Heat Mass Transfer* **13**(1970), 434–438 (1970).
28. Prasad, K. V., Vajravelu, K. & Datti, P. S. Mixed convection heat transfer over a non-linear stretching surface with variable fluid properties. *Int. J. Non-Linear Mech.* **45**(3), 320–330 (2010).
29. Jena, S., Dash, G. C. & Mishra, S. R. Chemical reaction effect on MHD viscoelastic fluid flow over a vertical stretching sheet with heat source/sink. *Ain Shams Eng. J.* **9**(4), 1205–1213 (2016).
30. Hayat, T., Qayyum, S., Alsaedi, A. & Ahmad, B. Magnetohydrodynamic (MHD) nonlinear convective flow of Walters-B nanofluid over a nonlinear stretching sheet with variable thickness. *Int. J. Heat Mass Transf.* **110**, 506–514 (2017).
31. Kumaran, G., Sivaraj, R., Prasad, V. R., Beg, O. A. & Sharma, R. P. Finite difference computation of free magneto-convective Powell-Eyring nanofluid flow over a permeable cylinder with variable thermal conductivity. *Phys. Scr.* **96**(2), 025222 (2000).

32. Nayak, M. K. MHD 3D flow and heat transfer analysis of nanofluid by shrinking surface inspired by thermal radiation and viscous dissipation. *Int. J. Heat Mass Transfer* **124**, 185 (2017).
33. Hsiao, K.-L. Mixed convection with radiation effect over a nonlinearly stretching sheet. *Int. J. Mech. Mechatron. Eng.* **4**(2), 164–168 (2010).
34. Reddy, N. N., Rao, V. S. & Reddy, B. R. Velocity slip, chemical reaction, and suction/injection effects on two-dimensional unsteady MHD mass transfer flow over a stretching surface in the presence of thermal radiation and viscous dissipation. *Heat Transfer* **51**(2), 1982–2002 (2022).
35. Yaseen, M., Rawat, S. K. & Kumar, M. Hybrid nanofluid (MoS2–SiO2/water) flow with viscous dissipation and Ohmic heating on an irregular variably thick convex/concave-shaped sheet in a porous medium. *Heat Transfer* **51**(1), 789–817 (2022).
36. Jahan, S., Ferdows, M., Shamshuddin, M. D. & Zaimi, K. Effects of solar radiation and viscous dissipation on mixed convective non-isothermal hybrid nanofluid over moving thin needle. *J. Adv. Res. Micro Nano Eng.* **3**(1), 1–11 (2021).
37. Cebeci, T. & Bradshaw, P. *Physical and Computational Aspects of Convective Heat Transfer* (Springer Science Business Media, 2012).
38. Kumaran, G. *et al.* Numerical study of axisymmetric magneto-gyrotactic bioconvection in non-Fourier tangent hyperbolic nano-functional reactive coating flow of a cylindrical body in porous media. *Eur. Phys. J. Plus* **136**(11), 1107 (2021).
39. Hayath, T. B., Ramachandran, S., Vallampati, R. P. & Bég, O. A. Computation of non-similar solution for magnetic pseudoplastic nanofluid flow over a circular cylinder with variable thermophysical properties and radiative flux. *Int. J. Numer. Methods Heat Fluid Flow* **2020**, 55 (2020).
40. Kumaran, G., Sivaraj, R., Prasad, V. R., Beg, O. A. & Sharma, R. P. Finite difference computation of free magneto-convective Powell-Eyring nanofluid flow over a permeable cylinder with variable thermal conductivity. *Phys. Scr.* **96**, 025222 (2021).
41. Goud, B. S. *et al.* Numerical case study of chemical reaction impact on MHD micropolar fluid flow past over a vertical riga plate. *Materials* **15**(12), 4060 (2022).
42. Zhao, T. H., Khan, M. I. & Chu, Y. M. Artificial neural networking (ANN) analysis for heat and entropy generation in flow of non-Newtonian fluid between two rotating disks. *Math. Methods Appl. Sci.* https://doi.org/10.1002/mma.7310 (2021).
43. Zhao, T. H., He, Z. Y. & Chu, Y. M. On some refinements for inequalities involving zero-balanced hypergeometric function. *AIMS Math.* **5**, 6479–6495 (2020).
44. Zhao, T. H., Wang, M. K. & Chu, Y. M. A sharp double inequality involving generalized complete elliptic integral of the first kind. *AIMS Math.* **5**, 4512–4528 (2020).
45. Chu, Y. M., Nazir, U., Sohail, M., Selim, M. M. & Lee, J. R. Enhancement in thermal energy and solute particles using hybrid nanoparticles by engaging activation energy and chemical reaction over a parabolic surface via finite element approach. *Fract. Fract.* **5**, 119 (2021).
46. Chu, Y. M., Bashir, S., Ramzan, M. & Malik, M. Y. Model-based comparative study of magnetohydrodynamics unsteady hybrid nanofluid flow between two infinite parallel plates with particle shape effects. *Math. Methods Appl. Sci.* **2022**, 5 (2022).
47. Zhao, T. H., Chu, H. H. & Chu, Y. M. Optimal Lehmer mean bounds for the nth power-type Toader mean of n=-1, 1, 3. *J. Math. Inequal.* **6**(1), 157–168 (2022).
48. Zhao, T. H., Wang, M. K., Dai, Y. Q. & Chu, Y. M. On the generalized power-type Toader mean. *J. Math. Inequal.* **16**(1), 247–264 (2022).
49. Iqbal, S. A., Hafez, M. G., Chu, Y. M. & Park, C. Dynamical Analysis of nonautonomous RLC circuit with the absence and presence of Atangana-Baleanu fractional derivative. *J. Appl. Anal. Comput.* **12**, 770–789 (2022).
50. Ashpazzadeh, E., Chu, Y. M., Hashemi, M. S., Moharrami, M. & Inc, M. Hermite multiwavelets representation for the sparse solution of nonlinear Abel's integral equation. *Appl. Math. Comput.* **427**, 127171 (2022).
51. Chu, Y. M. *et al.* Combined impact of Cattaneo-Christov double diffusion and radiative heat flux on bio-convective flow of Maxwell liquid configured by a stretched nano-material surface. *Appl. Math. Comput.* **419**, 126883 (2022).
52. Nazeer, M. *et al.* Theoretical study of MHD electro-osmotically flow of third-grade fluid in micro channel. *Appl. Math. Comput.* **420**, 126868 (2022).
53. Koulali, A. *et al.* Comparative study on effects of thermal gradient direction on heat exchange between a pure fluid and a nanofluid: Employing finite volume method. *Coatings* **11**(12), 1481 (2021).
54. Mahammed, A. B. *et al.* Thermal management of MHD nanofluid within porous C shaped cavity with undulated baffle. *J. Thermophys. Heat Transfer* **2021**, 5 (2021).
55. Hussain, S. M. & Jamshed, W. A comparative entropy based analysis of tangent hyperbolic hybrid nanofluid flow: Implementing finite difference method. *Int. Commun. Heat Mass Transfer* **129**, 105671 (2021).
56. Parvin, S. *et al.* The flow, thermal and mass properties of Soret-Dufour model of magnetized Maxwell nanofluid flow over a shrinkage inclined surface. *PLoS ONE* **17**(4), e0267148 (2022).
57. Jamshed, W. *et al.* Physical specifications of MHD mixed convective of Ostwald–de Waele nanofluids in a vented-cavity with inner elliptic cylinder. *Int. Commun. Heat Mass Transfer* **134**, 106038 (2022).
58. Hussain, S. M. *et al.* Chemical reaction and thermal characteristics of maxwell nanofluid flow-through solar collector as a potential solar energy cooling application: A modified Buongiorno's model. *Energy Env.* https://doi.org/10.1177/0958305X221088113 (2022).
59. Ullah, I. Heat transfer enhancement in Marangoni convection and nonlinear radiative flow of gasoline oil conveying Boehmite alumina and aluminum alloy nanoparticles. *Int. Commun. Heat Mass Transfer* **132**, 105920 (2022).
60. Ullah, I. Activation energy with exothermic/endothermic reaction and Coriolis force effects on magnetized nanomaterials flow through Darcy-Forchheimer porous space with variable features. *Waves Random Compl. Media* **2022**, 1–14 (2022).
61. Ullah, I., Hayat, T., Aziz, A. & Alsaedi, A. Significance of entropy generation and the Coriolis force on the three-dimensional non-Darcy flow of ethylene-glycol conveying carbon nanotubes (SWCNTs and MWCNTs). *J. Non-Equilib. Thermodyn.* **47**(1), 61–75 (2022).
62. Hussain, S. M. *et al.* Effectiveness of nonuniform heat generation (sink) and thermal characterization of a carreau fluid flowing across a nonlinear elongating cylinder: A numerical study. *ACS Omega* **7**, 25309 (2022).
63. Pasha, A. A. *et al.* Statistical analysis of viscous hybridized nanofluid flowing via Galerkin finite element technique. *Int. Commun. Heat Mass Transfer* **137**, 106244 (2022).
64. Hussain, S. M., Jamshed, W., Pasha, A. A., Adil, M. & Akram, M. Galerkin finite element solution for electromagnetic radiative impact on viscid Williamson two-phase nanofluid flow via extendable surface. *Int. Commun. Heat Mass Transfer* **137**, 106243 (2022).
65. Jamshed, W. *et al.* Solar energy optimization in solar-HVAC using Sutterby hybrid nanofluid with Smoluchowski temperature conditions: A solar thermal application. *Sci. Rep.* **12**, 11484 (2022).

Acknowledgements

Author contributions

Conceptualization: A.B.J. and S.S. Formal analysis: I.U. Investigation: W.J. and I.U. Methodology: A.R. and R.S. Software: I.U., W.J. and E.S.M.T.E.D. Re-Graphical representation and adding analysis of data: M.M.R. and M.R.E. Writing-original draft: A.B.J., S.S. and I.U. Convergence: M.M.R. Writing-review editing: A.A.P. and M.R.E. Numerical process breakdown: A.A.P. Re-modelling design: S.M.H. and M.R.E. Validation: S.M.H. and M.R.E. Writing-review editing: M.R.E. Furthermore, all the authors equally contributed to the writing and proofreading of the paper. All authors reviewed the manuscript.

Competing interests

The authors declare no competing interests.

Additional information

Correspondence and requests for materials should be addressed to W.J.

Reprints and permissions information is available at www.nature.com/reprints.

Publisher's note Springer Nature remains neutral with regard to jurisdictional claims in published maps and institutional affiliations.